

# Electrocatalytic Water Oxidation by a Monomeric Amidate-Ligated Fe(III)–Aqua Complex

Michael K. Coggins, Ming-Tian Zhang, Aaron K. Vannucci, Christopher J. Dares, and Thomas J. Meyer\*

Department of Chemistry, University of North Carolina at Chapel Hill, Chapel Hill, North Carolina 27599, United States

**S** Supporting Information

**ABSTRACT:** The six-coordinate Fe<sup>III</sup>-aqua complex [Fe<sup>III</sup>(dpaq)(H<sub>2</sub>O)]<sup>2+</sup> (**1**, dpaq is 2-[bis(pyridine-2-ylmethyl)]amino-*N*-quinolin-8-yl-acetamido) is an electrocatalyst for water oxidation in propylene carbonate–water mixtures. An electrochemical kinetics study has revealed that water oxidation occurs by oxidation to Fe<sup>V</sup>(O)<sup>2+</sup> followed by a reaction first order in catalyst and added water, respectively, with  $k_o = 0.035(4) \text{ M}^{-1} \text{ s}^{-1}$  by the single-site mechanism found previously for Ru and Ir water oxidation catalysts. Sustained water oxidation catalysis occurs at a high surface area electrode to give O<sub>2</sub> through at least 29 turnovers over an 15 h electrolysis period with a 45% Faradaic yield and no observable decomposition of the catalyst.

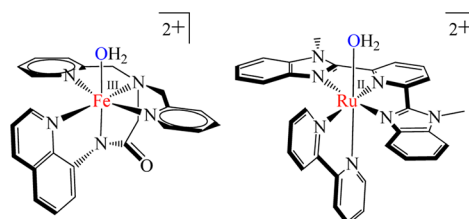


**Figure 1.** Structure of [Fe<sup>III</sup>(dpaq)(H<sub>2</sub>O)]<sup>2+</sup> (**1**, left) and [Ru<sup>II</sup>(Mebimpy)(bpy)(H<sub>2</sub>O)]<sup>2+</sup> (right).

Water oxidation is a key half reaction in natural photosynthesis and in most schemes for artificial photosynthesis. It presents a considerable mechanistic challenge given its multi-electron, multiproton character (2H<sub>2</sub>O → O<sub>2</sub> + 4H<sup>+</sup> + 4e<sup>-</sup>,  $E^\circ = 1.23 \text{ V vs NHE}$ ). Progress has been made in developing both homogeneous<sup>1</sup> and surface-bound<sup>2</sup> transition metal catalysts, especially those based on Ru and Ir complexes, but there is a continuing need for earth-abundant first row catalysts. Compared to metal-oxide clusters and materials,<sup>3</sup> molecular catalysts have the advantage of being readily modified by chemical synthesis and incorporated into molecular assemblies for energy conversion applications.

Progress has been made with first row transition metal catalysts including recent examples of Mn,<sup>4</sup> Fe,<sup>5</sup> Co,<sup>2a,c,e,6</sup> and Cu complexes.<sup>7</sup> Iron complexes are of particular interest given the ubiquity of Fe in redox cofactors and oxygen carrying metalloenzymes in biology.<sup>8</sup> It is also the first transition series congener of Ru with its extensive and well-developed water oxidation chemistry.<sup>1a–d,g–i,2b,d</sup> Water oxidation catalysis by single-site Fe complexes with tetra- and pentadentate macrocyclic ligands has been reported, but typically in strongly acidic solutions with under conditions that lead to catalyst decomposition.<sup>5</sup> Electrocatalytic water oxidation has not been reported.

We report here that the six-coordinate Fe<sup>III</sup>-aqua complex, [Fe<sup>III</sup>(dpaq)(H<sub>2</sub>O)](ClO<sub>4</sub>)<sub>2</sub> (**1**, dpaq is 2-[bis(pyridine-2-ylmethyl)]amino-*N*-quinolin-8-yl-acetamido, Figure 1), is an electrocatalyst for water oxidation in propylene carbonate with water added as a limiting reagent. Sustained water oxidation catalysis is observed in this medium and a detailed mechanism has been determined based on the results of cyclic voltammetry (CV) measurements. Similar to related Ru polypyridyl

complexes, the mechanism for water oxidation by **1** involves proton coupled electron transfer (PCET) oxidation to Fe<sup>V</sup>(O)<sup>2+</sup>, followed by rate limiting O-atom transfer to a neighboring water molecule.

Complex **1** was synthesized and characterized as its ClO<sub>4</sub><sup>-</sup> salt as previously described.<sup>9</sup> In 0.1 M HClO<sub>4</sub>,  $E_{1/2}$  values for the quasi-reversible Fe<sup>III</sup>(OH<sub>2</sub>)<sup>2+</sup>/Fe<sup>II</sup>(OH<sub>2</sub>)<sup>+</sup> and Fe<sup>IV</sup>(O)<sup>+</sup>/Fe<sup>III</sup>(OH<sub>2</sub>)<sup>2+</sup> couples appear at 0.24 and 1.19 V versus the normal hydrogen electrode (NHE), respectively (Supporting Information Figures S-1 and S-2). A pH-independent Fe<sup>V</sup>(O)<sup>2+</sup>/Fe<sup>IV</sup>(O)<sup>+</sup> wave appears at 1.52 V vs NHE (Supporting Information Figure S-1). Above pH 10.5, **1** decomposes to give an insoluble product (or products) that were not identified but which may be iron-hydroxide nanoparticles, as recently reported by Fukuzumi and co-workers in related complexes.<sup>5i</sup>

In order to explore the ability of **1** to serve as an electrocatalyst for water oxidation in aqueous solution, cyclic voltammetry (CV) experiments were performed at a glassy carbon electrode at pH 1 in 0.1 M HClO<sub>4</sub>, at pH 3.9 (0.01–0.1 M acetate buffer), and 7.1 (0.01–0.05 M phosphate buffer) each with a constant ionic strength of 0.5 M maintained with added LiClO<sub>4</sub>. A comparison of scan rate ( $\nu$ ) normalized CVs ( $i/\nu^{1/2}$ ) within the potential window 0.20 to 1.8 V versus NHE at scan rates from 10 mV/s to 300 mV/s revealed diffusion-controlled oxidation at the electrode and no clear evidence for a scan rate independent component arising from rate limiting catalysis (note the representative CVs in Supporting Information Figure S-3). On the basis of these results, there is no evidence in the CVs for water oxidation catalysis following oxidation of **1** to Fe<sup>V</sup>(O)<sup>2+</sup>, even at scan rates as low as 10 mV/s and with relatively high concentrations of added proton acceptor bases ([HPO<sub>4</sub><sup>2-</sup>] = 50 mM at pH = 7.1), which are conditions known to enhance water oxidation by atom-proton transfer (APT).<sup>10,11</sup>

**Received:** December 17, 2013

**Published:** March 26, 2014

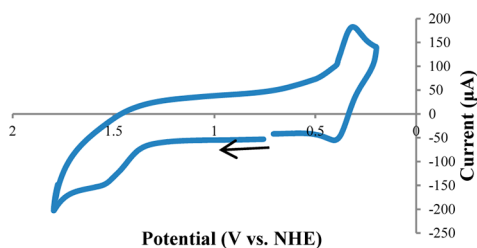


**Figure 2.** Cyclic voltammogram of  $[\text{Fe}^{\text{III}}(\text{dpaq})(\text{H}_2\text{O})](\text{ClO}_4)_2$  (**1**) (0.34 mM) in propylene carbonate (0.5 M  $\text{LiClO}_4$ ) at 50 mV/s at a glassy carbon working electrode (0.07  $\text{cm}^2$ ) at room temperature with the arrow indicating the initial scan direction.

Given the fact that a previous observation that the rate of water oxidation electrocatalysis by  $[\text{Ru}^{\text{II}}(\text{Mebimpy})(\text{bpy})(\text{H}_2\text{O})]^{2+}$  (Mebimpy is 2,6-bis(1-methylbenzimidazol-2-yl)pyridine and bpy is 2,2'-bipyridine, Figure 1) is accelerated in propylene carbonate (PC)/ $\text{H}_2\text{O}$  mixtures by a factor of 300 compared to acidic aqueous solution due to the loss in solvent stabilization of water in this medium,<sup>10</sup> CV measurements on **1** were extended to PC with added water. At room temperature, PC is an effective solvent for electrocatalytic water and hydrocarbon oxidation due to its relatively high miscibility with water (8% v/v) and weak coordinating ability.

CVs of **1** in dry PC (0.5 M  $\text{LiClO}_4$ ) exhibit a quasireversible one-electron wave corresponding to the  $\text{Fe}^{\text{III}}(\text{OH}_2)^{2+}/\text{Fe}^{\text{II}}(\text{OH}_2)^+$  couple at  $E_{1/2} = 0.38$  V vs NHE (Figure 2) with a peak-to-peak potential separation of  $\Delta E_p = 73$  mV and an anodic (oxidative) to cathodic (reductive) peak current ratio of  $i_{p,a}/i_{p,c} \approx 1$ . At higher potentials, an irreversible two-electron,  $\text{Fe}^{\text{III}}(\text{OH}_2)^{2+} \rightarrow \text{Fe}^{\text{V}}(\text{O})^{2+}$ , wave appears at  $E_{p,a} = 1.58$  V vs NHE (based upon relative currents passed, Figure 2). The increased current above background and absence of a discernible rereduction wave for the  $\text{Fe}^{\text{V}}(\text{O})^{2+}/\text{Fe}^{\text{III}}(\text{OH}_2)^{2+}$  couple point to solvent oxidation following oxidation to  $\text{Fe}^{\text{V}}(\text{O})^{2+}$ . Peak currents for both waves increased linearly with the square root of the scan rate ( $\nu^{1/2}$ ) from 10 to 500 mV/s consistent with diffusion-limited electron transfer at the electrode. There was no sign of precipitation or film formation on the working electrode. Following 70 CV scan cycles from 0.2 to 1.7 V vs NHE at 75 mV/s, CVs were indistinguishable and superimposable, consistent with the stability of the complex under these conditions.

Upon addition of water, there was an increase in current at the onset of the  $\text{Fe}^{\text{V}}(\text{O})^{2+}/\text{Fe}^{\text{III}}(\text{OH}_2)^{2+}$  wave (Figure 3). The magnitude of the peak current at 1.58 V vs NHE varied with  $[\text{H}_2\text{O}]^{1/2}$  up to the miscibility limit at 8% v/v (4.4 M). Controlled potential electrolysis (CPE) experiments were conducted at a high surface area reticulated vitreous carbon electrode coated with tin-doped indium oxide nanoparticles (*nano*ITO-RVC,<sup>12</sup> RVC area = 16.5  $\text{cm}^2$ ) at 1.58 V vs NHE with 0.2 mM **1** in PC/8%  $\text{H}_2\text{O}$  solutions (0.5 M  $\text{LiClO}_4$ , Figure 4). Background current densities in the absence of **1** were 1–2  $\mu\text{A cm}^{-2}$  over the same time interval (Supporting Information Figure S-4). Following the electrolysis period, the reaction headspace was sampled for  $\text{O}_2$  and analyzed by gas chromatography/mass spectrometry. In a typical experiment, 29  $\mu\text{mol}$  of  $\text{O}_2$  were produced over a 15 h electrolysis period corresponding to a 45% Faradaic efficiency through 29 catalyst turnovers (Figure 4).

$\text{CO}_2$  was not detected in any significant quantity as an electrolysis product in the reaction headspace with or without added **1**, suggesting that the *nano*ITO-RVC working electrodes

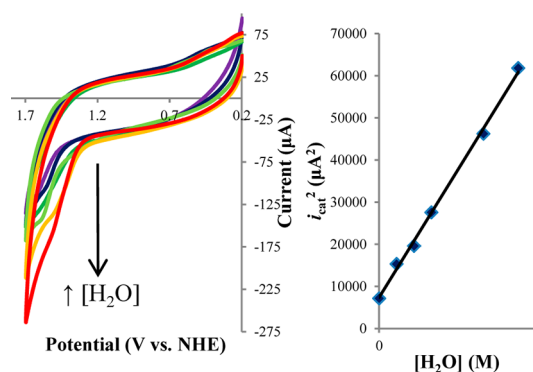


**Figure 3.** (Left) Cyclic voltammograms of  $[\text{Fe}^{\text{III}}(\text{dpaq})(\text{H}_2\text{O})](\text{ClO}_4)_2$  (**1**) (0.2 mM) in propylene carbonate (0.5 M  $\text{LiClO}_4$ ) at 75 mV/s with increasing amounts of  $\text{H}_2\text{O}$  (GC working electrode, 0.07  $\text{cm}^2$ , room temperature). (Right) Plot of  $i_{\text{cat}}^2$  (background subtracted) at 1.58 V vs NHE versus  $[\text{H}_2\text{O}]$ .

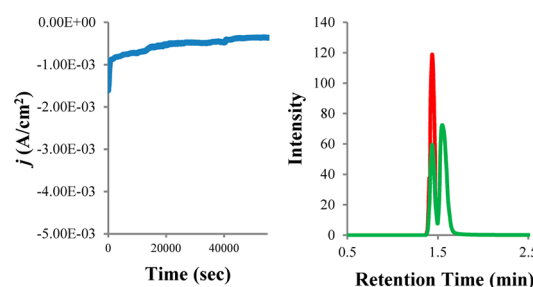


**Figure 4.** (Left) Current density-time controlled potential electrolysis (CPE) plot for  $[\text{Fe}^{\text{III}}(\text{dpaq})(\text{H}_2\text{O})](\text{ClO}_4)_2$  (**1**) (0.2 mM) in propylene carbonate/8%  $\text{H}_2\text{O}$  v/v (0.5 M  $\text{LiClO}_4$ ) at 1.58 V vs NHE (background subtracted, *nano*ITO-RVC, 16.5  $\text{cm}^2$ ). (Right) Gas chromatograms of the headspace from the CPE experiment in the presence (red trace) and absence (green trace) of **1**.

are not oxidized under the conditions of the experiments. The excess current appears to arise from background propylene carbonate oxidation, as propylene carbonate is known to undergo both oxidation and hydrolysis to give a wide variety of products.<sup>13</sup> Background solvent oxidation was of less importance in an earlier study based on a Ru polypyridyl complex in propylene carbonate due to the complex being much more reactive toward water.<sup>10</sup> Little decomposition of **1** was found to occur during the CPE experiment, as shown by UV–vis and CV measurements before and after electrolysis (Supporting Information Figure S-5,6). The stability of **1** under these conditions with oxygen evolution is impressive compared to earlier results with related Fe macrocyclic complexes in acidic solutions with added  $\text{Ce}^{\text{IV}}$  or periodate as oxidants.<sup>5</sup>

The peak current at 1.58 V vs NHE was found to vary linearly with catalyst concentration,  $[\mathbf{1}]$ , at a glassy carbon electrode at 75 mV/s in PC/8%  $\text{H}_2\text{O}$  (0.5 M  $\text{LiClO}_4$ , Figure 5). The peak current variations with  $[\mathbf{1}]$  and  $[\text{H}_2\text{O}]$  are consistent with the rate law in eq 1 and the expression for the catalytic current ( $i_{\text{cat}}$ ) in eq 2 and a rate limiting reaction between  $\text{Fe}^{\text{V}}(\text{O})^{2+}$  and  $\text{H}_2\text{O}$ . In eqs 1 and 2,  $k_{\text{cat}}$  is the catalytic rate constant,  $k_o$  is the second order rate constant for the reaction between  $\text{Fe}^{\text{V}}(\text{O})^{2+}$  and  $\text{H}_2\text{O}$ ,  $n$  is the number of electrons transferred with  $n_{\text{cat}} = 4$  for water oxidation,  $F$  is the Faraday constant,  $A$  is the area of the working electrode ( $\text{cm}^2$ ), and  $D_{\text{Fe}}$  is the diffusion coefficient of the catalyst  $\text{cm}^2/\text{sec}$ . The rate law in eq 1 is consistent with a single site mechanism for water oxidation as observed previously for a

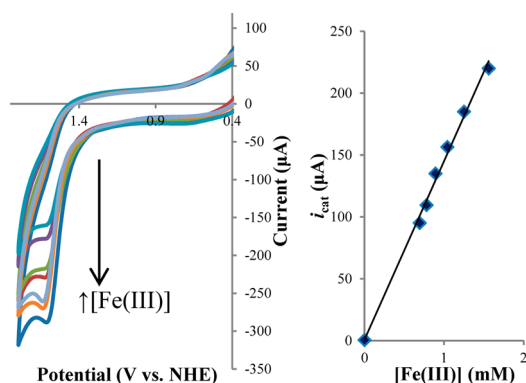


**Figure 5.** (Left) Cyclic voltammograms (75 mV/s) of  $[\text{Fe}^{\text{III}}(\text{dpaq})(\text{H}_2\text{O})](\text{ClO}_4)_2$  (**1**) with increasing concentrations of **1** (designated by black arrow) in propylene carbonate/4%  $\text{H}_2\text{O}$  v/v (0.5 M  $\text{LiClO}_4$ ) at a glassy carbon working electrode and room temperature. (Right) Plot of catalytic current ( $i_{\text{cat}}$ ) at 1.58 V vs NHE versus the concentration of **1** ( $[\text{Fe}(\text{III})]$ ) with background subtraction.

family of Ru polypyridyl water oxidation catalysts<sup>1d,h</sup> rather than a bimolecular mechanism with  $\text{Fe}^{\text{V}}(\text{O})\cdots(\text{O})\text{Fe}^{\text{V}}$  oxo-oxo coupling.<sup>1c</sup>

$$\text{rate} = k_{\text{cat}}[\text{Fe}^{\text{V}}=\text{O}] = k_0[\text{Fe}^{\text{V}}=\text{O}][\text{H}_2\text{O}] \quad (1)$$

$$i_{\text{cat}} = n_{\text{cat}}FA[\text{Fe}](k_{\text{cat}}D_{\text{Fe}})^{1/2} = nFA[\text{Fe}](k_0[\text{H}_2\text{O}]D_{\text{Fe}})^{1/2} \quad (2)$$

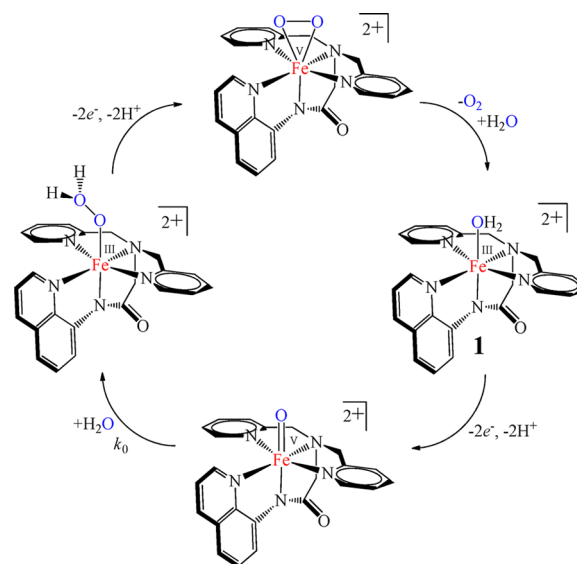
The kinetics of water oxidation were investigated by scan rate-dependent CV measurements with 1.0 mM **1** in a PC/8%  $\text{H}_2\text{O}$  solution 0.5 M in  $\text{LiClO}_4$  at a GC working electrode (Supporting Information Figure S-7). Catalytic currents at 1.58 V vs NHE ( $i_{\text{cat}}$ ) were normalized to the cathodic  $\text{Fe}^{\text{III/II}}$  wave at 0.34 V vs NHE ( $i_p$ ) and fit to the expression in eq 4, which follows from eq 2 and the Randles–Sevcik relation in eq 3 (where  $n = 1$ ). In eq 4,  $R$  is the ideal gas constant,  $T$  is the temperature, and  $\nu$  is the scan rate.

$$i_p = 0.4633nFA[\mathbf{1}](nF\nu D_{\text{Fe}}/RT)^{1/2} \quad (3)$$

$$\begin{aligned} i_{\text{cat}}/i_p &= 2.242(k_0RT[\text{H}_2\text{O}]/(nF\nu))^{1/2} \\ &= 2.242([k_{\text{cat}}RT]/(nF\nu))^{1/2} \end{aligned} \quad (4)$$

From the slope of the plot of  $i_{\text{cat}}/i_p$  vs  $\nu^{-1/2}$  in Supporting Information Figure S-8,  $k_0 = 0.035(4) \text{ M}^{-1} \text{ s}^{-1}$  ( $k_{\text{cat}} = 0.15(3) \text{ sec}^{-1}$ ,  $[\text{H}_2\text{O}] = 4.4 \text{ M}$ ). This value is more than an order of magnitude slower than the rate constant for water oxidation by  $[\text{Ru}^{\text{V}}(\text{Mebimpy})(\text{bpy})(\text{O})]^{3+}$  with  $k_{\text{cat}} \approx 1 \text{ s}^{-1}$  under the same conditions.<sup>10</sup> CV experiments were also conducted with added  $\text{D}_2\text{O}$  rather than  $\text{H}_2\text{O}$  (Supporting Information Figure S-9). Analysis of these data gave  $k_{\text{O},\text{D}_2\text{O}} = 0.032 \text{ M}^{-1} \text{ sec}^{-1}$  with a  $\text{H}_2\text{O}/\text{D}_2\text{O}$  kinetic isotope effect (KIE,  $k_{\text{O},\text{H}_2\text{O}}/k_{\text{O},\text{D}_2\text{O}}$ ) of 1.08. This is in contrast to KIE = 6.6 for the oxidation of water by  $[\text{Ru}^{\text{V}}(\text{tpy})(\text{bpm})(\text{O})]^{3+}$  (tpy is 2,2':6',2''-terpyridine; bpm is 2,2'-bipyrimidine)<sup>11</sup> The isotope effect in water has been attributed to atom-proton transfer (APT) with O–O bond formation occurring in concert with proton transfer to a second water molecule or water cluster.<sup>11</sup> A reaction first order in  $[\text{H}_2\text{O}]$  and the absence of a significant KIE points to a mechanism involving O–O bond formation to generate the peroxide intermediate in Scheme 1. Even though water oxidation is slower by a factor of 10 than for  $[\text{Ru}^{\text{V}}(\text{Mebimpy})(\text{bpy})(\text{O})]^{3+}$  in

### Scheme 1. Proposed Mechanism for Electrocatalytic Water Oxidation by $[\text{Fe}^{\text{III}}(\text{dpaq})(\text{H}_2\text{O})](\text{ClO}_4)_2$ (**1**) in Propylene Carbonate/Water



PC, it is notable that the onset of catalytic current for water oxidation by **1** occurs at a 200–250 mV lower overpotential.<sup>9</sup>

The available experimental evidence in PC/ $\text{H}_2\text{O}$  points to the water oxidation mechanism in Scheme 1, which is analogous to the scheme found earlier for a series of Ru polypyridyl catalysts.<sup>1,10,11</sup> In this scheme, the catalytically active  $\text{Fe}^{\text{V}}(\text{O})^{2+}$  is obtained by PCET oxidative activation of  $\text{Fe}^{\text{III}}(\text{H}_2\text{O})^{2+}$ . Once formed, the reactive  $\text{Fe}^{\text{V}}(\text{O})^{2+}$  form of the catalyst reacts with  $\text{H}_2\text{O}$  by rate-limiting O–O bond formation to give an intermediate peroxide, presumably as  $\text{Fe}^{\text{III}}(\text{OOH}_2)^{2+}$ , with a KIE = 1.08. Following this rate-limiting step, further PCET oxidation of  $d^5 \text{Fe}^{\text{III}}(\text{OOH}_2)^{2+}$  to  $d^3 \text{Fe}^{\text{V}}(\text{OO})^{2+}$  may occur followed by rapid  $\text{O}_2$  release and  $\text{H}_2\text{O}$  coordination to reform **1** and re-enter the catalytic cycle. The rate advantage of using propylene carbonate as the solvent for catalytic water oxidation arises from the decreased stabilization of water.<sup>14</sup> There is no direct experimental evidence for either proposed  $\text{Fe}^{\text{III}}$ -peroxide intermediate or for free  $\text{H}_2\text{O}_2$ . Evidence has been obtained for peroxide intermediates in water oxidation by Ru polypyridyl catalysts in solution and, for phosphonate derivatives, on oxide surfaces.<sup>1,2,10,11</sup>

Our results are important in providing the first experimental example of well-defined water oxidation electrocatalysis by a molecular Fe complex. Water oxidation occurs by a single-site mechanism analogous to a mechanism established earlier for analogous Ru polypyridyl oxidants.<sup>1,10,11</sup> These results are also notable for the stability of the catalyst in the PC/water solvent mixture with multiple turnovers free of catalyst decomposition. The absence of significant reactivity toward water oxidation in aqueous solution over an extended pH range is disappointing with no evidence for catalysis on the CV time scale, even at slow scan rates and high concentrations of added  $\text{HPO}_4^{2-}$  buffer base. This is due, in part, to the lower oxidizing strength of the  $\text{Fe}^{\text{V}}(\text{O})^{2+}/\text{Fe}^{\text{III}}(\text{H}_2\text{O})^{2+}$  couple relative to the  $\text{Ru}^{\text{V}}(\text{O})^{2+}/\text{Ru}^{\text{III}}(\text{H}_2\text{O})^{2+}$  couple for  $[\text{Ru}(\text{Mebimpy})(\text{bpy})(\text{OH}_2)]^{2+}$ , for example, with the lower overpotential for water oxidation coming at the expense of decreased driving force for the key O–O bond forming step. The oxidative stability and long catalytic lifetime of **1** under these conditions are unprecedented relative to



other molecular Fe water oxidation catalysts, providing inspiration for the design of additional robust first row transition metal complexes for possible applications in electrocatalysis and photoelectrocatalysis.

## ■ ASSOCIATED CONTENT

### ■ Supporting Information

Experimental methods, aqueous cyclic voltammograms, UV–vis absorption spectra from controlled potential electrolysis, kinetics plots, background electrochemical data are presented. This material is available free of charge via the Internet at <http://pubs.acs.org>.

## ■ AUTHOR INFORMATION

### Corresponding Author

tjmeyer@unc.edu

### Notes

The authors declare no competing financial interest.

## ■ ACKNOWLEDGMENTS

Funding by the Center for Catalytic Hydrocarbon Functionalization, an Energy Frontier Research Center (EFRC), funded by the U.S. Department of Energy (DOE), Office of Science, Office of Basic Energy Sciences, under Award DE-SC0001298 is gratefully acknowledged for supporting M.K.C. Funding by the UNC EFRC Solar Fuels, an EFRC funded by the U.S. DOE, Office of Science, Office of Basic Energy Sciences, under Award DE-SC0001011 is gratefully acknowledged for supporting M.-T.Z. and A.K.V.

## ■ REFERENCES

- (1) (a) Gersten, S. W.; Samuels, G. J.; Meyer, T. J. *J. Am. Chem. Soc.* **1982**, *104*, 4029–4030. (b) Zong, R.; Thummel, R. P. *J. Am. Chem. Soc.* **2005**, *127*, 12802–12803. (c) McDaniel, N. D.; Coughlin, F. J.; Tinker, L. L.; Bernhard, S. *J. Am. Chem. Soc.* **2008**, *130*, 210–217. (d) Concepcion, J. J.; Jurss, J. W.; Templeton, J. L.; Meyer, T. J. *J. Am. Chem. Soc.* **2008**, *130*, 16462–16463. (e) Betley, T. A.; Wu, Q.; Van Voorhis, T.; Nocera, D. G. *Inorg. Chem.* **2008**, *47*, 1849–1861. (f) Hull, J. F.; Balcells, D.; Blakemore, J. D.; Incarvito, C. D.; Eisenstein, O.; Brudvig, G. W.; Crabtree, R. H. *J. Am. Chem. Soc.* **2009**, *131*, 8730–8731. (g) Duan, L.; Fischer, A.; Xu, Y.; Sun, L. *J. Am. Chem. Soc.* **2009**, *131*, 10397–10399. (h) Concepcion, J. J.; Jurss, J. W.; Norris, M. R.; Chen, Z.; Templeton, J. L.; Meyer, T. J. *Inorg. Chem.* **2010**, *49*, 1277–1279. (i) Ashford, D. L.; Stewart, D. J.; Glasson, C. R.; Binstead, R. A.; Harrison, D. P.; Norris, M. R.; Concepcion, J. J.; Fang, Z.; Templeton, J. L.; Meyer, T. J. *Inorg. Chem.* **2012**, *51*, 6428–6430. (j) Norris, M. R.; Concepcion, J. J.; Harrison, D. P.; Binstead, R. A.; Ashford, D. L.; Fang, Z.; Templeton, J. L.; Meyer, T. J. *J. Am. Chem. Soc.* **2013**, *135*, 2080–2083.
- (2) (a) Kanan, M. W.; Nocera, D. G. *Science* **2008**, *321*, 1072–1075. (b) Chen, Z.; Concepcion, J. J.; Jurss, J. W.; Meyer, T. J. *J. Am. Chem. Soc.* **2009**, *131*, 15580–15581. (c) Surendranath, Y.; Kanan, M. W.; Nocera, D. G. *J. Am. Chem. Soc.* **2010**, *132*, 16501–16509. (d) Chen, Z.; Vannucci, A. K.; Concepcion, J. J.; Jurss, J. W.; Meyer, T. J. *Proc. Natl. Acad. Sci. U. S. A.* **2011**, *108*, E1461–E1469. (e) Nocera, D. G. *Acc. Chem. Res.* **2012**, *45*, 767–776. (f) Costi, R.; Young, E. R.; Bulovic, V.; Nocera, D. G. *ACS Appl. Mater. Interfaces* **2013**, *5*, 2364–2367. (g) Blakemore, J. D.; Mara, M. W.; Kushner-Lenhoff, M. N.; Schley, N. D.; Konezny, S. J.; Rivalta, I.; Negre, C. F. A.; Snoeberger, R. C.; Kokhan, O.; Huang, J.; Stickrath, A.; Tran, L. A.; Parr, M. L.; Chen, L. X.; Tiede, D. M.; Batista, V. S.; Crabtree, R. H.; Brudvig, G. W. *Inorg. Chem.* **2013**, *52*, 1860–1871. (h) Hong, D.; Yamada, Y.; Nomura, A.; Fukuzumi, S. *Phys. Chem. Chem. Phys.* **2013**, *15*, 19125–19128.
- (3) (a) Cavka, J. H.; Jakobsen, S.; Olsbye, U.; Guillou, N.; Lamberti, C.; Bordiga, S.; Lillerud, K. P. *J. Am. Chem. Soc.* **2008**, *130*, 13850–13851.

- (b) Wang, C.; Xie, Z.; deDrafft, K. E.; Lin, W. *J. Am. Chem. Soc.* **2011**, *133*, 13445–13454. (c) Wang, C.; Wang, J.-L.; Lin, W. *J. Am. Chem. Soc.* **2012**, *134*, 19895–19908. (d) Joya, K. S.; Subbaiyan, N. K.; D'Souza, F.; de Groot, H. J. M. *Angew. Chem., Int. Ed.* **2012**, *51*, 9601–9605. (e) Nepal, B.; Das, S. *Angew. Chem., Int. Ed.* **2013**, *52*, 7224–7227.
- (4) (a) Ashmawy, F. M.; McAuliffe, C. A.; Parish, R. V.; Tames, J. J. *Chem. Soc., Dalton Trans.* **1985**, 1391–1397. (b) Watkinson, M.; Whiting, A.; McAuliffe, C. A. *J. Chem. Soc., Chem. Comm.* **1994**, 2141–2142. (c) Limburg, J.; Vrettos, J. S.; Liable-Sands, L. M.; Rheingold, A. L.; Crabtree, R. H.; Brudvig, G. W. *Science* **1999**, *283*, 1524–1527. (d) Tagore, R.; Crabtree, R. H.; Brudvig, G. W. *Inorg. Chem.* **2008**, *47*, 1815–1823. (e) Gao, Y.; Akermark, T.; Liu, J.; Sun, L.; Akermark, B. *J. Am. Chem. Soc.* **2009**, *131*, 8726–8727. (f) Dismukes, G. C.; Brimblecombe, R.; Felton, G. A. N.; Prydun, R. S.; Sheats, J. E.; Spiccia, L.; Swiegers, G. F. *Acc. Chem. Res.* **2009**, *42*, 1935–1943. (g) Young, K. J.; Takase, M. K.; Brudvig, G. W. *Inorg. Chem.* **2013**, *52*, 7615–7622.
- (5) (a) Ellis, W. C.; McDaniel, N. D.; Bernhard, S.; Collins, T. J. *J. Am. Chem. Soc.* **2010**, *132*, 10990–10991. (b) Fillol, J. L.; Codola, Z.; Garcia-Bosch, I.; Gomez, L.; Pla, J. J.; Costas, M. *Nat. Chem.* **2011**, *3*, 807–813. (c) Garcia-Bosch, I.; Codola, Z.; Prat, I.; Ribas, X.; Lloret-Fillol, J.; Costas, M. *Chem.—Eur. J.* **2012**, *18*, 13269–13273. (d) Ertem, M. Z.; Gagliardi, L.; Cramer, C. J. *Chem. Sci.* **2012**, *3*, 1293–1299. (e) Sarma, R.; Angeles-Boza, A. M.; Brinkley, D. W.; Roth, J. P. *J. Am. Chem. Soc.* **2012**, *134*, 15371–15386. (f) Hong, D.; Yamada, Y.; Nagatomi, T.; Takai, Y.; Fukuzumi, S. *J. Am. Chem. Soc.* **2012**, *134*, 19572–19575. (g) Chen, G.; Chen, L.; Ng, S.-M.; Man, W.-L.; Lau, T.-C. *Angew. Chem., Int. Ed.* **2013**, *52*, 1789–1791. (h) Codola, Z.; Garcia-Bosch, I.; Acuña-Parés, F.; Prat, I.; Luis, J. M.; Costas, M.; Fillol-Lloret, J. *Chem.—Eur. J.* **2013**, *19*, 8042–8047. (i) Hong, D.; Mandal, S.; Yamada, Y.; Lee, Y.-M.; Nam, W.; Llobet, A.; Fukuzumi, S. *Inorg. Chem.* **2013**, *52*, 9522–9531.
- (6) (a) Wasylenko, D. J.; Ganesamoorthy, C.; Borau-Garcia, J.; Berlinguette, C. P. *Chem. Commun.* **2011**, *47*, 4249–4251. (b) Lai, W.; Cao, R.; Dong, G.; Shaik, S.; Yao, J.; Chen, H. *J. Phys. Chem. Lett.* **2012**, *3*, 2315–2319. (c) Pizzolato, E.; Natali, M.; Posocco, B.; López, A. M.; Bazzan, I.; Valentin, M. D.; Galloni, P.; Conte, V.; Bonchio, M.; Scandola, F.; Sartorel, A. *Chem. Commun.* **2013**, *49*, 9941–9943. (d) Wang, D.; Groves, J. T. *Proc. Natl. Acad. Sci. U. S. A.* **2013**, *110*, 15579–15584. (e) Han, A.; Wu, H.; Sun, Z.; Jia, H.; Du, P. *Phys. Chem. Chem. Phys.* **2013**, *15*, 12534–12538. (f) Wasylenko, D. J.; Tatlock, H. M.; Bhandari, L. S.; Gardinier, J. R.; Berlinguette, C. P. *Chem. Sci.* **2013**, *4*, 734–738.
- (7) (a) Barnett, S. M.; Goldberg, K. I.; Mayer, J. M. *Nat. Chem.* **2012**, *4*, 498–502. (b) Chen, Z.; Meyer, T. J. *Angew. Chem., Int. Ed.* **2013**, *52*, 700–703. (c) Zhang, M.-T.; Chen, Z.; Kang, P.; Meyer, T. J. *J. Am. Chem. Soc.* **2013**, *135*, 2048–2051. (d) Chen, Z.; Kang, P.; Zhang, M.-T.; Stoner, B. R.; Meyer, T. J. *Energy Environ. Sci.* **2013**, *6*, 813–817.
- (8) (a) Sono, M.; Roach, M. P.; Coulter, E. D.; Dawson, J. H. *Chem. Rev.* **1996**, *96*, 2841–2888. (b) Costas, M.; Mehn, M. P.; Jensen, M. P.; Que, L., Jr. *Chem. Rev.* **2004**, *104*, 939–986. (c) Denisov, I. G.; Makris, T. M.; Sligar, S. G.; Schlichting, I. *Chem. Rev.* **2005**, *105*, 2253–2277.
- (9) Hitomi, Y.; Arakawa, K.; Funabiki, T.; Kodera, M. *Angew. Chem., Int. Ed.* **2012**, *51*, 3448–3452.
- (10) Chen, Z.; Concepcion, J. J.; Luo, H.; Hull, J. F.; Paul, A.; Meyer, T. J. *J. Am. Chem. Soc.* **2010**, *132*, 17670–17673.
- (11) Chen, Z.; Concepcion, J. J.; Hu, X.; Yang, W.; Hoertz, P. G.; Meyer, T. J. *Proc. Natl. Acad. Sci. U. S. A.* **2010**, *107*, 7225–7229.
- (12) For the use of nanoITO-RVC electrodes for controlled potential electrolysis experiments, see Méndez, M. A.; Alibabaei, L.; Concepcion, J. J.; Meyer, T. J. *ACS Catal.* **2013**, *3*, 1850–1854.
- (13) For examples of propylene carbonate oxidation/hydrolysis products, see (a) Rasch, B.; Cattaneo, E.; Novák, P.; Vielstich, W. *Electrochim. Acta* **1991**, *36*, 1397–1402. (b) Hlavatý, J.; Novák, P. *Electrochim. Acta* **1992**, *37*, 2595–2597. (c) Ufheil, J.; Würsig, A.; Schneider, O. D.; Novák, P. *Electrochim. Commun.* **2005**, *7*, 1380–1384. (d) Laino, T.; Curioni, A. *Chem.—Eur. J.* **2012**, *18*, 3510–3520.
- (14) (a) Muzikar, J.; van de Goor, T.; Gaš, B.; Kennler, E. *Anal. Chem.* **2002**, *74*, 428–433. (b) Cantu, M. D.; Hillebrand, S.; Carrillo, E. J. *J. Chromatogr., A* **2005**, *1068*, 99–105.